Conference on Modelling Fluid Flow (CMFF'25)
The 19th International Conference on Fluid Flow Technologies
Budapest, Hungary, August 26 - August 29, 2025

A NOVEL SPH MODEL FOR THROMBUS FORMATION

Sumanta LAHA[1,2], Georgios FOURTAKAS[1], Prasanta.K. DAS[2], Amir KESMIRI[1,3]

[1] Corresponding Author. School of Engineering, The University of Manchester, M13 9PL, UK E-mail: sumanta.laha@manchester.ac.uk
[2] Department of Mechanical Engineering, Indian Institute of Technology Kharagpur, India
[3] Manchester University NHS Foundation Trust, Manchester, M13 9PL, UK. E-mail: a.keshmiri@manchester.ac.uk

ABSTRACT

Cardiovascular diseases remain a major global health challenge, often driven by uncontrolled thrombus formation. A comprehensive understanding of its biochemical, biological, and mechanical mechanisms is crucial. Due to the complexities and limitations of in-vivo studies, computational fluid dynamics (CFD) has emerged as a viable and cost-effective alternative. This research presents a novel smoothed particle hydrodynamics (SPH)-based methodology for modelling thrombus formation and growth. Optimised for graphics processing unit (GPU) execution, the approach significantly reduces computational time for thrombus simulations. Two distinct thrombus growth strategies—the penalty approach and the dissipation approach—are investigated to determine the most effective method. The penalty approach incorporates a fibrin-linked velocity penalty term, while the dissipation approach integrates the Einstein equation with fibrin concentration. The model captures the coagulation cascade by simulating key biochemical components, including thrombin, prothrombin, fibrinogen, fibrin, and both activated and resting platelets. The implementation utilises the DualSPHysics solver, incorporating wall shear stress effects to enhance thrombus modelling. To validate the model, simulations were performed in a backward-facing step, demonstrating the effectiveness of SPH in predicting device-induced thrombosis. This study offers a promising step toward advancing cardiovascular research and improving clinical outcomes.

Keywords: Thrombosis, Thrombus formation, Coagulation cascade, Thrombin, Fibrin, DualSPHysics, GPU, CFD, Smoothed particle hydrodynamics.

NOMENCLATURE

Due to space constraints, only a selection of key nomenclature used in this study is provided below.

Biochemical Parameters		
C_{th}	[M]	Thrombin concentration
C_{fb}	[M]	Fibrin concentration
C_{pt}	[M]	Prothrombin concentration
C_{rp}	[PLT ml^{-1}]	Resting platelet concentration
C_{ap}	[PLT ml^{-1}]	Activated platelet concentration
k_{th}	[UPLT^{-1}s^{-1}μM^{-1}]	Thrombin generation rate constant
τ	[Pa]	Wall shear stress

1. INTRODUCTION

Thrombosis is a major contributor to cardiovascular diseases, as it can obstruct blood flow within vessels, potentially leading to life-threatening emergencies by restricting circulation to vital organs. The symptoms vary depending on the clot's location and may include chest pain, breathing difficulties, and skin discoloration, as well as severe conditions like stroke, pulmonary embolism, or ictus. According to Virchow's triad [1], three primary factors contribute to vascular thrombosis: increased blood coagulability, altered blood flow (stasis), and damage to the vessel wall or endothelium. The process of thrombus formation, also known as the coagulation cascade, involves a series of complex biochemical reactions. It is primarily initiated through two pathways—the intrinsic and extrinsic pathways—which eventually converge in the coagulation process. In vascular injury, subendothelial cells become exposed to blood flow, and prolonged exposure triggers biochemical interactions between tissue factors and blood cells, leading to platelet activation and adhesion. Simultaneously, the coagulation cascade is activated, promoting fibrin formation, which stabilizes the clot and facilitates thrombus growth.

Over the years, extensive efforts have been devoted to understanding the intricate mechanisms underlying thrombus formation, drawing from both

fluid mechanics and chemical kinetics. Given the complexity of this process, numerical methods, including semi-empirical and computational modelling, play a crucial role in gaining a macroscopic understanding of thrombus formation.

Computational fluid dynamics (CFD) has emerged as a powerful tool for integrating the hydrodynamics of blood flow with biochemical reactions, building on the success of computational techniques in analysing and predicting haemodynamics in various cardiovascular diseases and medical devices [2]–[5]. While research in this field is not new, its continued importance drives ongoing efforts to refine existing models and develop novel methodologies. Leiderman and Fogelson [6] were pioneers in developing an early spatiotemporal mathematical model for platelet aggregation and blood coagulation under flow conditions. Their model provides a comprehensive framework for understanding coagulation biochemistry, chemical activation, platelet deposition, and the dynamic interaction between fluid dynamics and the growing platelet mass. In a similar vein, Govindarajan et al. [7] introduced an innovative model designed to simulate thrombus formation under venous flow conditions. After validating their model against the work of Colace et al. [8], they further explored the hydraulic resistance caused by platelets and thrombus, offering valuable insights into the complex interactions within the bloodstream.

Particle tracking and time history are crucial for thrombus modelling and are well-suited to the Lagrangian description of motion. Additionally, fluid-structure interaction (FSI) between thrombus, blood, and the cardiovascular vessel plays a key role in accurately simulating thrombus growth and its subsequent breakdown. Recently, there has been an increasing trend in using particle-based Lagrangian approaches for modelling thrombus formation. Tsubota et al. [9] investigated thrombus formation following Fontan surgery using a moving particle semi-implicit scheme. In their model, thrombus formation and attachment were governed by shear rate thresholds and spring attraction forces. While other simplified particle-based models, which consider thrombus shells as thrombin species, exist, they fail to incorporate biochemical reactions.

In recent years, meshless methods, particularly Smoothed Particle Hydrodynamics (SPH), have gained traction as effective tools for simulating cardiovascular haemodynamics [10], [11]. Chui et al. [12] applied SPH to develop a basic clotting model based on local shear rate, where clotting begins in areas subjected to shear stress below a certain threshold. Al Saad et al. [13] advanced SPH modelling by describing thrombus formation with platelet adhesion and aggregation, utilising elastic forces dependent on the distance from an injured vessel. Wang et al. [14] built on this by introducing biochemical reactions and a velocity decay term linked to fibrin concentration. However, focusing solely on fibrin presents a potential limitation. More recently, Monteleone et al. [15] presented an SPH model incorporating various biochemical factors like thrombin, prothrombin, fibrin, and activated platelets. This model used convection-diffusion equations to estimate primary concentrations and switching functions based on threshold concentrations to simulate platelet activation. Upon reaching a critical concentration of bound platelets, particles transition to solid form, mimicking thrombus formation. However, this model overlooks advection terms, wall shear stress in thrombus modelling, and the gradual reduction of platelet velocity in response to rising fibrin concentrations.

The current study proposes a novel methodology based on SPH to model thrombus formation, accumulation, and growth, addressing the limitations of Monteleone et al.'s model [15]. The key innovation lies in combining SPH nearest-neighbour searching to simulate platelet activation with the mesh-like effects of fibrin networks. This approach also incorporates advanced modelling techniques to capture particle deposition within the thrombus. Two unique approaches are employed: a penalty approach, which applies a velocity penalty term based on fibrin concentration to simulate restriction effects, and a dissipation approach, where fibrin concentration is linked to the Einstein equation to introduce an additional dissipation term. To further enhance the model, wall shear stress from recent work is integrated to couple mechanical influences with biochemical processes. A novel method has been introduced to dynamically activate and drive the model based on wall shear stress. The methodology has been rigorously validated against experimental data, including thrombus formation. The more detailed work of the thrombus modelling could be found in the recent publication from same authors [16].

2. MATERIAL AND METHODS

In this section, a brief description of the SPH formulation is provided. In SPH, the continuous approximation of a scalar field function $A(r)$ at a point r in a one-dimensional domain is expressed in by integral representation, written as:

$$A(r) := \int W(r - r', h) A(r')\, d\omega \tag{1}$$

where W is a smoothing function or smoothing kernel, h is the smoothing length in the support domain of the kernel function and ω is the volume of the integral.

The discrete form of Eq. (1) can be written as,

$$A_i = \sum_j^N W(r_i - r_i, h) A_j\, V_j \tag{2}$$

where ω is discretized into N computational nodes or particles. Here, i and j represent the interpolating and neighbouring particles,

respectively, and V is the volume of the particle, defined as $V = m/\rho$, with m being the mass and ρ the density of the particle.

The choice of a smoothing function directly impacts the solution. Various smoothing kernels are available in the literature [17]. In this work, Wendland C^2 kernel has been selected due to its higher-order (5th) nature, which allows it to capture higher-order effects with improved accuracy [17]. The Wendland kernel is defined as follows [18],

$$W(r,h) = \begin{cases} \alpha_d \left(1-\frac{q}{2}\right)^4 (2q+1), & 0 \le q \le 2 \\ 0 & q > 2 \end{cases} \quad (3)$$

where $q = |r_{ij}|/h$ and α_d is $\frac{3}{4h}$, $\frac{7}{4\pi h^2}$, $\frac{21}{16\pi h^3}$ for 1D, 2D, and 3D, respectively. For further information on the SPH method, the reader is directed to [19] and [20].

The governing equations for the haemodynamics are the mass and momentum conservation. To solve these equations, the domain is discretised, and approximate values for the field functions are calculated at specific points. Throughout the SPH simulation, the mass of each particle is kept constant while the density of the particles changes according to the continuity equation. The general form of the continuity equation is as follows,

whereas the SPH discrete form of Eq. (4) can take the following form [21],

$$\frac{\mathrm{D}\rho}{\mathrm{Dt}} = -\rho \nabla \cdot (\mathbf{u}) \quad (4)$$

$$\frac{\mathrm{D}\rho}{\mathrm{Dt}} = \rho_i \sum_{j \in P} \frac{m_j}{\rho_j} (\mathbf{u}_i - \mathbf{u}_j) \cdot \nabla W_{ij} \quad (5)$$

where $\mathbf{u}$ is the velocity of the particle and t denotes physical time. Herein, i and j denote the interpolating and neighbouring particles respectively and $P = F \cup B$ where F and B denote the fluid and boundary particles respectively.

The momentum conservation equation can be written as,

$$\frac{\mathrm{D}\mathbf{u}}{Dt} = -\frac{1}{\rho}\nabla p + \Gamma + \mathbf{f} \quad (6)$$

where p is the pressure, Γ is the dissipative term and $\mathbf{f}$ represents external forces. In SPH notation, Eq. (6) can be expressed as,

$$\frac{\mathrm{D}\mathbf{u}}{\mathrm{Dt}} = -\sum_{j \in P} \left(\frac{p_i + p_j}{\rho_i \rho_j}\right) \nabla W_{ij} m_j + \langle \Gamma \rangle + \mathbf{f} \quad (7)$$

The above equation satisfies the momentum conservation.

Instead of the widely used artificial viscosity scheme, a combination of Shao and Lo operators a large eddy Sub-Particle Scale (SPS) [22] turbulence model has been used in the present study as described by Dalrymple and Rogers [23] to define the dissipation term. In this scheme, the momentum equation is given by,

$$\frac{\mathrm{D}\mathbf{u}}{\mathrm{Dt}} = -\frac{1}{\rho}\nabla p + \mathbf{g} + \nu \nabla^2 \mathbf{u} + \frac{1}{\rho}\nabla \cdot \boldsymbol{\tau} \quad (8)$$

where $\nu\nabla^2\mathbf{u}$ is the laminar viscous stress and it can be expressed as [24],

$$(\nu \nabla^2 \mathbf{u})_i = \sum_{j \in P} m_j \left(\frac{4\nu \mathbf{r_{ij}} \cdot \nabla_i W_{ij}}{(\rho_i + \rho_j) + (r_{ij}^2 + 0.01h^2)}\right) \mathbf{u}_{ij} \quad (9)$$

The last term in the right-hand side of Eq. (8) is accounted for by the SPS stress tensor and that term can be expressed by the means of Favre averaging which is generally used to compute compressibility in weakly compressible SPH [23]. The term is as follows,

$$\frac{1}{\rho}\nabla \cdot \tau_i^{\alpha\beta} = \sum_{j \in P} m_j \left(\frac{\tau_i^{\alpha\beta} + \tau_j^{\alpha\beta}}{\rho_i \rho_j}\right) \cdot \nabla_i W_{ij} \quad (10)$$

here, τ is the SPS stress tensor and has been defined in Einstein notation over superscripts α and β (spatial coordinates).

Therefore, the momentum Eq. (8) can be expressed in SPH terms by,

$$\frac{\mathrm{D}u_i^a}{\mathrm{Dt}} = -\sum_{j \in P} \left(\frac{p_i + p_j}{\rho_i \rho_j}\right) \frac{\partial W_{ij}}{\partial x_i^\alpha} m_j + \mathrm{f}_i^a + \sum_{j \in P} m_j \left(\frac{4\nu r_{ij}^\beta \frac{\partial W_{ij}}{\partial x_i^\beta} W_{ij}}{(\rho_i + \rho_j) + (r_{ij}^2 + 0.01h^2)}\right) u_{ij}^a + \sum_{j \in P} m_j \left(\frac{\tau_i^{\alpha\beta} + \tau_j^{\alpha\beta}}{\rho_i \rho_j}\right) \frac{\partial W_{ij}}{\partial x_i^\beta} W_{ij} \quad (11)$$

Most of the hydrodynamic problems can be approximated by the weakly compressible SPH (WCSPH) scheme. To compute the fluid pressure based on the density of the particle, an equation of state (EOS) is employed, and by regulating the compressibility, the speed of sound is kept artificially low. As a result, the numerical speed of sound is restricted to be at least ten times the speed of the maximum velocity of the system which retains the density variation to less than 1%. This resembles closely an incompressible flow approach.

In the present study, Tait's EOS is used [25], [26] which is given by,

$$P = \frac{c^2 \rho_0}{\gamma} \left(\left(\frac{\rho}{\rho_0} \right)^{\gamma} - 1 \right), \quad (12)$$

where $\gamma = 7$ is the polytrophic index, ρ_0 is the density of the reference fluid at the beginning of the simulation, and the c is the speed of sound at the reference density. In the present work the smoothing length has been taken 1.7 times of the particle spacing and the viscosity of the fluid has been chosen like blood which is 3cP.

2.1. Physiology of the thrombus formation

The key physical processes involved in thrombus formation, which will be incorporated into the present model, are outlined below. Thrombus formation begins with primary haemostasis, where a platelet plug is formed, followed by the activation of the coagulation cascade. When vascular injury occurs, the exposure of collagen initiates this process.

Vasoconstriction: The initial response to vascular injury involves the constriction of blood vessels, reducing blood flow to the affected area.

Platelet plug formation: Platelets adhere to the exposed collagen at the injury site, become activated, and aggregate to form a temporary plug that helps prevent further blood loss.

Activation of the coagulation cascade: Once primary haemostasis is established, the coagulation cascade is triggered, leading to secondary haemostasis.

Final clot formation: As the coagulation cascade progresses, fibrin concentration increases, reinforcing the clot with a dense fibrin network. This marks the final stage of thrombus formation. Eventually, after tissue repair is complete, fibrinolysis occurs, breaking down and dissolving the clot.

2.2. Modelling of the thrombus formation

The modelling process begins with identifying damaged zones where high wall shear stress ($\tau_h > 10Pa$) is activating platelets on a damaged vessel surface, and low wall shear stress ($\tau_l < 0.02Pa$) promotes platelet adhesion and accumulation. Fluid particles within a distance of $2h$ (smoothing radius) from the damaged wall are considered contributors to thrombus formation. Prothrombin concentration reduces with thrombin formation, governed by an advection-diffusion equation (Eq. 13) Following the methodology proposed by Monteleone et al. [15], a source term has been selected based on the chemical kinetics.

$$\frac{\partial C_k}{\partial \mathrm{t}} = \nabla \cdot (D_k \nabla C_k) - \nabla \cdot (\mathbf{u_k} C_k) + R_k \quad (13)$$

where C is the concentration of the bio-chemical species, D is the diffusion coefficient, $\mathbf{u}$ is the velocity of the particle and R is the respective source term. Eq. (13) has been solved for prothrombin, thrombin, fibrin and activated platelet respectively. The above equation discretised and computed through SPH approximation. The SPH version of the equation for a particular species is as follows, where i and j represent the interpolating and neighbouring particles, respectively,

The source term for the prothrombin and thrombin are as follows,

$$\frac{\partial C_i}{\partial \mathrm{t}} = \sum_{j \epsilon P} m_j \left(\frac{4 D_i \mathbf{r_{ij}} \cdot \nabla_i W_{ij}}{(\rho_i + \rho_j) + (r_{ij}^2 + 0.01h^2)} \right) C_{ij} + C_i \sum_{j \epsilon P} \frac{m_j}{\rho_j} (\mathbf{u}_i - \mathbf{u}_j) \cdot \nabla W_{ij} + \mathbf{u}_{\mathrm{i}} \sum_{j \epsilon P} \frac{m_j}{\rho_{\mathrm{j}}} (C_i - C_j) \cdot \nabla W_{ij}, \quad + R_i \quad (14)$$

$$R_{th} = k_{th}^{rp} C_{rp} C_{pt} + k_{th}^{ap} C_{ap} C_{pt} \quad (15)$$

$$R_{pt} = -R_{th} \quad (16)$$

where k_{th}^{rp} and k_{th}^{ap} is the kinetic constant of the resting and activated platelets for the thrombin conversation from the prothrombin. C_{rp}, C_{ap}, C_{pt} are the concentration of the resting platelet, activated platelet and prothrombin, respectively.

When thrombin concentration of a particle exceeds a threshold (C_{th_th}), they are considered as activated platelets. Biochemical interactions between prothrombin, thrombin, and fibrin, governed by Michaelis-Menten kinetics, drive this process, while activated platelets are drawn toward the wall or nearby activated platelets, promoting aggregation.

In the final mechanistic step, velocities of the particles must be reduced based on the fibrin concentration. In the penalty approach, a velocity penalty term proposed by Wang et al. [14] has been introduced,

$$u_{penalty} = \beta \left(1 - \left(\frac{C_{fb,i}}{C_{fb,i}, th} \right)^{1.5} \right) \quad (17)$$

Here $C_{fb,i}$ is the concentration of the fibrin of the interpolating particle and β is a penalty factor considered 1 in the present case. This term gradually reduces particle velocity depending on fibrin concentration, ultimately setting it to rest.

$$\mathbf{u_{i\_new}} = \mathbf{u_i}\, u_{penalty} \quad (18)$$

Table 1. Details of the computational hardware and simulation parameters

Hardware	Geometry domain	No of particle	Run Time
NVIDIA RTX V100 GPU	120×10×10mm (L × B × H)	60,550	40 min
		317,818	4 hours
		1,072,832	32 hours

It has been demonstrated that reasonable prediction of thrombus formation is achieved based on the above modelling technique. However, the gradual decrease in local velocity during fibrin formation is based on an empirical penalty function. This gradual decrease in velocity is due to the deposition of fibrin being similar to fluid flow with dispersion where the viscosity may be predicted through Einstein constitutive equation. Therefore, in the dissipation approach, an additional viscous term is proposed. In the momentum equation the kinematic viscosity ν has been replaced by ν_c by using the Einstein constitutive equation for the viscosity, thus

where φ is an arbitrary constant tuned based on the initial fluid viscosity and has a value of $O(10)^{12}$, sufficiently large to bring the fluid to a complete stop. Therefore, the modified momentum equation based on Eq. (8) can be written as,

$$\frac{\mathrm{D}\mathbf{u}}{\mathrm{D}t} = -\frac{1}{\rho}\nabla p + \mathbf{f} + \nu\nabla^2\mathbf{u} + \left(C_{fb,i}\varphi\right)\nabla^2\mathbf{u} + \frac{1}{\rho}\nabla.\boldsymbol{\tau} \tag{19}$$

Evidently, while the concentration of fibrin (i.e. the fibrin mesh) increases, the term ν_c rises, leading to the deposition of the particles. This approach aligns closely with the physics of clot formation, as the fibrin mesh captures more platelets and reduces flow velocity, supporting the final clot formation. Thereafter, at the final stage while the concentration of the fibrin exceeds a threshold, velocity of the particles is set to zero.

2.3. Implementation and Hardware Acceleration

In this study, the thrombus model has been implemented in DualSPHysics [27], an open-source, C++-based code that leverages graphics processing unit (GPU) hardware acceleration. The code utilises the WCSPH formulation, as discussed in sub sections 2.1 and 2.2. The modified dynamic boundary condition (mDBC) proposed by English et al. [28] has been applied in all the validation test cases. For a more detailed explanation of the boundary condition implementation, please refer to [28]. Given that thrombosis is a time-intensive phenomenon, relying solely on CPU-based models can be impractical due to prolonged simulation runtimes. To enhance computational efficiency, the thrombus model in this study has been specifically designed and optimised for execution on GPUs. All simulations were conducted using the University of Manchester's Computational Sharing Facility (CSF3) with NVIDIA RTX V100 GPUs.

Validation test case was performed in a 3D backward-facing step (BFS) [29]. A detailed description of these test cases is provided in Section 3. Additionally, Table 1 presents the computational time required to run the 3D BFS test cases at different resolutions, illustrating the average simulation runtime of the thrombus model.

3. RESULTS AND DISCUSSIONS

Generally, direct validation of any thrombus model is challenging due to the limited availability of experimental data. Nevertheless, in the present work, the efficacy of the proposed model is demonstrated through case study as validation basis. considering thrombus formation in a backward-facing step geometry as proposed by Taylor et al. [29].

Here, a three-dimensional backward-facing step has been chosen for the thrombus formation. This is a common configuration in fluid dynamics to study flow recirculation, separation and attachment, all of

$$\nu_c = (1 + C_{fb,i}\varphi)\nu \tag{20}$$

which are favourable for the thrombus formation. Moreover, this test case is one of the popular benchmark test cases for the validation of the thrombus model. A geometry of the BFS proposed by Taylor et al. [29] has been reconstructed as depicted in Fig. 1 (side view). A steady flow of 0.2 m/s has been prescribed at the inlet, while the outlet is kept at a zero constant pressure. More detailed parameters for this case study could be found in [16].

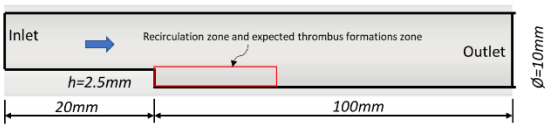

Figure 1. Schematic diagram of the fluid domain of the backward facing step test case.

3.1. Penalty Approach

Using the penalty approach, Fig. 2 illustrates that thrombus formation begins at the step corner and expands both axially and radially. The maximum thrombus length is ten times the step height, aligning with the findings of Taylor et al. [29]. The top view

of the thrombus in BFS geometry, resembling an expanding triangle, is compared in Fig. 2 with the experimental data from Taylor et al. [29], showing good agreement.

Fig. 4 further validates the proposed model quantitatively by comparing thrombus height, length, and surface area over time. The model accurately predicts thrombus length, as also visually confirmed in Fig. 2. However, while the SPH model closely matches the experimental thrombus shape and length at the 5th time instant, it tends to slightly over-predict experimental results qualitatively. In terms of thrombus height and exposed surface area, the model's predictions align well with the experimental data from Taylor et al. [29].

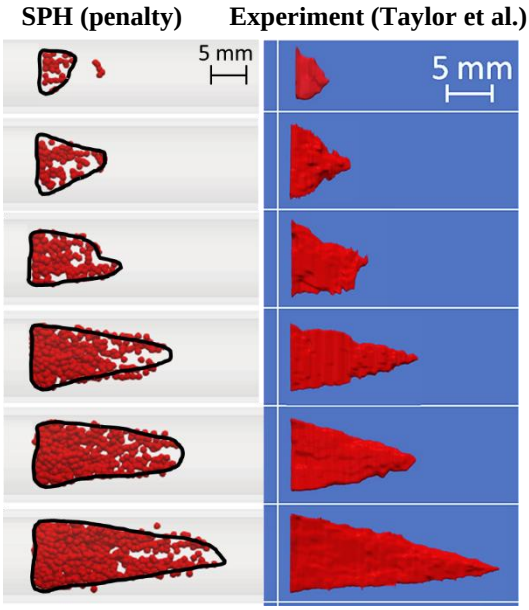

Figure 2. Comparison of predicted thrombus shape in the BFS geometry against the experimental observation by Taylor et al. using the penalty approach at different times

Nevertheless, at the 4th and 5th time instants, the simulated thrombus height slightly exceeds the experimental error range, with an estimated deviation of 5%. A similar deviation is observed for the exposed surface area. These results highlight the accuracy and reliability of the proposed model. It is important to note that this model represents an accelerated approach to thrombus formation, designed to reduce computational runtime. This expedited methodology is inspired by similar approaches found in the existing literature [15].

3.2. Dissipation approach

After successfully implementing the penalty approach for thrombus modelling using the velocity penalty term, an alternative dissipation approach was explored. As previously discussed, this method is more physiologically relevant, incorporating an additional fibrin-linked dissipation term based on Einstein's viscosity equation. The same test on the BFS geometry was repeated using the dissipation approach, while maintaining identical boundary conditions.

As shown in Fig. 3, the dissipation approach reasonably predicts thrombus shapes, though some noise in the form of unwanted random particles—absent in the penalty approach—is observed due to numerical instabilities. The thrombus shapes predicted by the dissipation approach are slightly more compressed radially than those obtained using the penalty approach, resulting in a closer match with experimental observations [29].

For quantitative validation, the thrombus length, height, and surface area predicted by the dissipation approach were compared with experimental results from Taylor et al. [29], as shown in Fig. 4. While the predicted thrombus length closely matches or slightly overestimates the initial model's results, the height and surface area are slightly underestimated, aligning more closely with experimental data. This highlights the improved accuracy of the dissipation approach.

It is important to note that, while the dissipation approach provides more physically accurate results, it is computationally demanding. Unlike the penalty approach, which employs a straightforward velocity reduction mechanism with small time-steps, the dissipation approach incorporates an additional viscous dissipation term, significantly increasing computational costs. Furthermore, the coefficient in Einstein's viscosity equation plays a crucial role and must be carefully calibrated before implementation. Despite these challenges, when properly executed, the dissipation approach enhances the accuracy of thrombus modelling

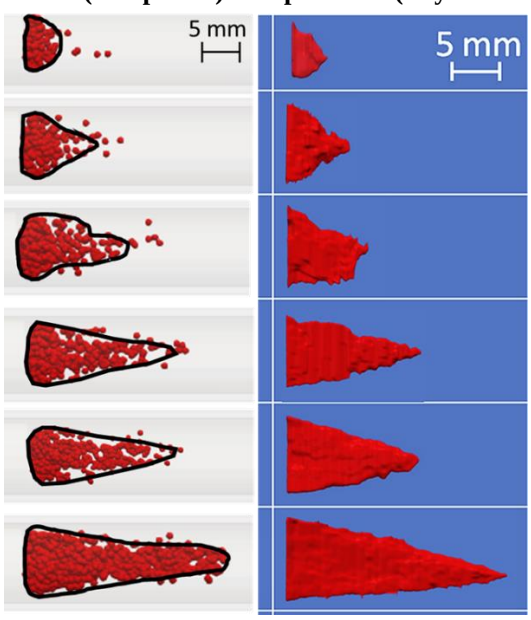

Figure 3. Comparison of predicted thrombus shape in the BFS geometry against the

experimental observation by Taylor et al. using the dissipation approach at different times

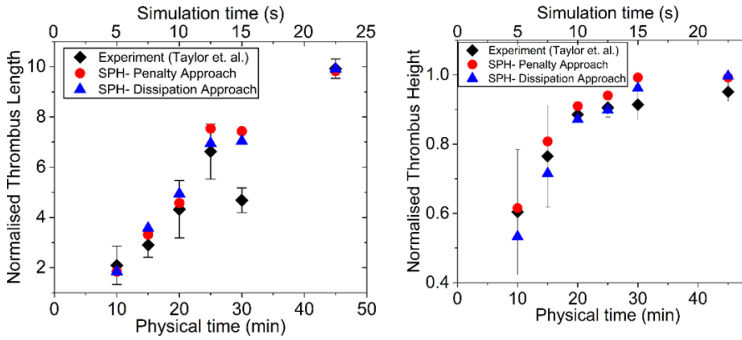

Figure 4. Comparison of the length height, and the surface area of the thrombus shape in the BFS geometry predicted by the present model against the experimental observation by Taylor et al. The length and height have been normalised by the step height

4. CONCLUSION

This study presents a novel SPH-based computational model for thrombus formation, integrating biochemical reactions and fluid dynamics to capture key aspects of clot development. A unique platelet activation and aggregation mechanism, implemented through the nearest neighbours searching method, enhances the model's physiological accuracy. Two distinct velocity reduction approaches were introduced: an empirical velocity penalty term and a physics-driven dissipation method based on Einstein's viscosity equation. While both approaches effectively simulate thrombus formation, the dissipation method provides improved accuracy by incorporating a more realistic representation of fibrin-linked dissipation. The model successfully replicates thrombus formation in pressure-driven microchannels and a backward-facing step, demonstrating strong agreement with experimental observations in terms of thrombus size, shape, and surface area. However, the complexity of thrombus formation necessitates certain simplifications. One key limitation is the high computational cost, which scales with resolution, requiring a scaled-down time frame rather than real physical time- a common trade-off in similar studies. Despite these limitations, the model demonstrates the potential of SPH in simulating thrombus formation in complex geometries where traditional mesh-based methods face challenges. Its ability to predict device-induced thrombosis further highlights its relevance for cardiovascular research and medical applications. Future work will focus on enhancing the model's physiological accuracy by incorporating initial pathway reactions, antithrombin dynamics, and a more refined treatment of clot evolution, ultimately improving its applicability in biomedical simulations.

ACKNOWLEDGEMENTS

The first author would like to acknowledge the Ph.D. funding under the 'Dual Doctoral Programme with the IIT Kharagpur' awarded by the University of Manchester. The underpinning research in this work has also been supported by the UKRI Engineering and Physical Sciences Research Council (EPSRC), under the grant EP/M015599/

REFERENCES

[1] R. Virchow, *Gesammelte abhandlungen zur wissenschaftlichen medicin*. BoD--Books on Demand, 2022.

[2] M. Mcelroy *et al.*, "Identification of the haemodynamic environment permissive for plaque erosion," *Sci. Rep.*, pp. 1–10, 2021, doi: 10.1038/s41598-021-86501-x.

[3] A. Keshmiri and K. Andrews, "Vascular Flow Modelling Using Computational Fluid Dynamics," in *Handbook of Vascular Biology Techniques*, 2015. doi: 10.1007/978-94-017-9716-0.

[4] A. Ruiz-Soler, F. Kabinejadian, M. M. A. Slevin, P. J. P. J. Bartolo, and A. Keshmiri, "Optimisation of a Novel Spiral-Inducing Bypass Graft Using Computational Fluid Dynamics," *Sci. Rep.*, vol. 7, no. 1, 2017, doi: 10.1038/s41598-017-01930-x.

[5] M. McElroy, A. Xenakis, and A. Keshmiri, "Impact of heart failure severity on ventricular assist device haemodynamics: a computational study," *Res. Biomed. Eng.*, vol. 36, no. 4, pp. 489–500, 2020, doi: 10.1007/s42600-020-00088-2.

[6] K. Leiderman and A. L. Fogelson, "Grow with the flow: A spatial-temporal model of platelet deposition and blood coagulation under flow," *Math. Med. Biol.*, vol. 28, no. 1, pp. 47–84, 2011,

[7] V. Govindarajan, V. Rakesh, J. Reifman, and A. Y. Mitrophanov, "Computational Study of Thrombus Formation and Clotting Factor Effects under Venous Flow Conditions," *Biophys. J.*, vol. 110, no. 8, pp. 1869–1885,

2016, doi: 10.1016/j.bpj.2016.03.010.
[8] T. V Colace, R. W. Muthard, and S. L. Diamond, “Thrombus growth and embolism on tissue factor-bearing collagen surfaces under flow: Role of thrombin with and without fibrin,” *Arterioscler. Thromb. Vasc. Biol.*, vol. 32, no. 6, pp. 1466 – 1476, 2012, doi: 10.1161/ATVBAHA.112.249789.
[9] K. I. Tsubota, K. Sughimoto, K. Okauchi, and H. Liu, “Particle method simulation of thrombus formation in fontan route,” *Model. Simul. Sci. Eng. Technol.*, pp. 387–396, 2016, doi: 10.1007/978-3-319-40827-9_30.
[10] S. Laha, G. Fourtakas, P. K. Das, and A. Keshmiri, “Fluid-Structure Interaction Modelling of Bi-Leaflet Mechanical Heart Valves Using Smoothed Particle Hydrodynamics,” *Phys. Fluids*, pp. 1–24, 2023, doi: 10.1063/5.0172043.
[11] S. Laha, G. Fourtakas, P. K. Das, and A. Keshmiri, “Smoothed particle hydrodynamics based FSI simulation of the native and mechanical heart valves in a patient-specific aortic model,” *Sci. Rep.*, vol. 14, no. 1, pp. 1–18, 2024, doi: 10.1038/s41598-024-57177-w.
[12] Y. P. Chui and P. A. Heng, “A meshless rheological model for blood-vessel interaction in endovascular simulation,” *Prog. Biophys. Mol. Biol.*, vol. 103, no. 2–3, pp. 252–261, 2010,
[13] M. Al-Saad, C. A. Suarez, A. Obeidat, S. P. A. Bordas, and S. Kulasegaram, “Application of smooth particle hydrodynamics method for modelling blood flow with thrombus formation,” *C. - Comput. Model. Eng. Sci.*, vol. 122, no. 3, pp. 831–862, 2020, doi: 10.32604/cmes.2020.08527.
[14] F. Wang *et al.*, “Particle hydrodynamic simulation of thrombus formation using velocity decay factor,” *Comput. Methods Programs Biomed.*, vol. 207, p. 106173, 2021, doi: 10.1016/j.cmpb.2021.106173.
[15] A. Monteleone, A. Viola, E. Napoli, and G. Burriesci, “Modelling of thrombus formation using smoothed particle hydrodynamics method,” *PLoS One*, vol. 18, no. 2 February, pp. 1–24, 2023, doi: 10.1371/journal.pone.0281424.
[16] S. Laha, G. Fourtakas, P. K. Das, and A. Keshmiri, “Graphics processing unit accelerated modeling of thrombus formation in cardiovascular systems using smoothed particle hydrodynamics,” *Phys. Fluids*, vol. 37, no. 2, 2025, doi: 10.1063/5.0250640.
[17] W. Dehnen and H. Aly, “Improving convergence in smoothed particle hydrodynamics simulations without pairing instability,” *Mon. Not. R. Astron. Soc.*, vol. 425, no. 2, pp. 1068–1082, 2012,
[18] H. Wendland, “Piecewise polynomial, positive definite and compactly supported radial functions of minimal degree,” *Adv. Comput. Math.*, vol. 4, no. 1, pp. 389–396, 1995, doi: 10.1007/BF02123482.
[19] D. Violeau and B. D. Rogers, “Smoothed particle hydrodynamics (SPH) for free-surface flows: past, present and future,” *J. Hydraul. Res.*, vol. 54, no. 1, pp. 1–26, 2016, doi: 10.1080/00221686.2015.1119209.
[20] D. Violeau, *Fluid Mechanics and the SPH Method*. Oxford University Press, 2012.
[21] A. J. C. Crespo *et al.*, “DualSPHysics: Open-source parallel CFD solver based on Smoothed Particle Hydrodynamics (SPH),” *Comput. Phys. Commun.*, vol. 187, pp. 204–216, 2015, doi: 10.1016/j.cpc.2014.10.004.
[22] H. Gotoh, T. Shibahara, and T. Sakai, “Sub-particle-scale turbulence model for the MPS method - Lagrangian flow model for hydraulic engineering,” *Comput. Fluid Dyn. J.*, vol. 9, no. 4, pp. 339 – 347, 2001,
[23] R. A. Dalrymple and B. D. Rogers, “Numerical modeling of water waves with the SPH method,” *Coast. Eng.*, vol. 53, no. 2–3, pp. 141–147, 2006, doi: 10.1016/j.coastaleng.2005.10.004.
[24] E. Y. M. Lo and S. Shao, “Simulation of near-shore solitary wave mechanics by an incompressible SPH method,” *Appl. Ocean Res.*, vol. 24, no. 5, pp. 275–286, 2002, doi: 10.1016/S0141-1187(03)00002-6.
[25] C.Batchelor and G. K. Batchelor, *An introduction to fluid dynamics*. Cambridge university press, 2000.
[26] J. J. Monaghan, R. A. F. Cas, A. M. Kos, and M. Hallworth, “Gravity currents descending a ramp in a stratified tank,” *J. Fluid Mech.*, vol. 379, pp. 39 – 70, 1999, doi: 10.1017/s0022112098003280.
[27] J. M. Domínguez *et al.*, “DualSPHysics: from fluid dynamics to multiphysics problems,” *Comput. Part. Mech.*, vol. 9, no. 5, pp. 867–895, 2022, doi: 10.1007/s40571-021-00404-2.
[28] A. English *et al.*, “Modified dynamic boundary conditions (mDBC) for general-purpose smoothed particle hydrodynamics (SPH): application to tank sloshing, dam break and fish pass problems,” *Comput. Part. Mech.*, vol. 9, no. 5, pp. 1–15, 2022, doi: 10.1007/s40571-021-00403-3.
[29] J. O. Taylor *et al.*, “In vitro quantification of time dependent thrombus size using magnetic resonance imaging and computational simulations of thrombus surface shear stresses,” *J. Biomech. Eng.*, vol. 136, no. 7, pp. 1–11, 2014, doi: 10.1115/1.4027613.